Branching fractions for $Y(3S) \rightarrow \pi^{0}h_{b}$ and $\psi(2S) \rightarrow \pi^{0}h_{c}$

J. Y. Ge *et al.* (CLEO Collaboration)

Branching fractions for $\Upsilon(3S) \to \pi^0 h_b$ and $\psi(2S) \to \pi^0 h_c$

J. Y. Ge,[1] D. H. Miller,[1] I. P. J. Shipsey,[1] B. Xin,[1] G. S. Adams,[2] J. Napolitano,[2] K. M. Ecklund,[3] J. Insler,[4]
H. Muramatsu,[4] C. S. Park,[4] L. J. Pearson,[4] E. H. Thorndike,[4] S. Ricciardi,[5] C. Thomas,[6,5] M. Artuso,[7] S. Blusk,[7]
R. Mountain,[7] T. Skwarnicki,[7] S. Stone,[7] L. M. Zhang,[7] G. Bonvicini,[8] D. Cinabro,[8] A. Lincoln,[8] M. J. Smith,[8]
P. Zhou,[8] J. Zhu,[8] P. Naik,[9] J. Rademacker,[9] D. M. Asner,[10,*] K. W. Edwards,[10] K. Randrianarivony,[10]
G. Tatishvili,[10,*] R. A. Briere,[11] H. Vogel,[11] P. U. E. Onyisi,[12] J. L. Rosner,[12] J. P. Alexander,[13] D. G. Cassel,[13]
S. Das,[13] R. Ehrlich,[13] L. Gibbons,[13] S. W. Gray,[13] D. L. Hartill,[13] B. K. Heltsley,[13] D. L. Kreinick,[13]
V. E. Kuznetsov,[13] J. R. Patterson,[13] D. Peterson,[13] D. Riley,[13] A. Ryd,[13] A. J. Sadoff,[13] X. Shi,[13] W. M. Sun,[13]
J. Yelton,[14] P. Rubin,[15] N. Lowrey,[16] S. Mehrabyan,[16] M. Selen,[16] J. Wiss,[16] J. Libby,[17] M. Kornicer,[18]
R. E. Mitchell,[18] C. M. Tarbert,[18] D. Besson,[19] T. K. Pedlar,[20] D. Cronin-Hennessy,[21] J. Hietala,[21] S. Dobbs,[22]
Z. Metreveli,[22] K. K. Seth,[22] A. Tomaradze,[22] T. Xiao,[22] L. Martin,[6] A. Powell,[6] and G. Wilkinson[6]

(CLEO Collaboration)

[1] *Purdue University, West Lafayette, Indiana 47907, USA*
[2] *Rensselaer Polytechnic Institute, Troy, New York 12180, USA*
[3] *Rice University, Houston, Texas 77005, USA*
[4] *University of Rochester, Rochester, New York 14627, USA*
[5] *STFC Rutherford Appleton Laboratory, Chilton, Didcot, Oxfordshire, OX11 0QX, UK*
[6] *University of Oxford, Oxford OX1 3RH, UK*
[7] *Syracuse University, Syracuse, New York 13244, USA*
[8] *Wayne State University, Detroit, Michigan 48202, USA*
[9] *University of Bristol, Bristol BS8 1TL, UK*
[10] *Carleton University, Ottawa, Ontario, Canada K1S 5B6*
[11] *Carnegie Mellon University, Pittsburgh, Pennsylvania 15213, USA*
[12] *University of Chicago, Chicago, Illinois 60637, USA*
[13] *Cornell University, Ithaca, New York 14853, USA*
[14] *University of Florida, Gainesville, Florida 32611, USA*
[15] *George Mason University, Fairfax, Virginia 22030, USA*
[16] *University of Illinois, Urbana-Champaign, Illinois 61801, USA*
[17] *Indian Institute of Technology Madras, Chennai, Tamil Nadu 600036, India*
[18] *Indiana University, Bloomington, Indiana 47405, USA*
[19] *University of Kansas, Lawrence, Kansas 66045, USA*
[20] *Luther College, Decorah, Iowa 52101, USA*
[21] *University of Minnesota, Minneapolis, Minnesota 55455, USA*
[22] *Northwestern University, Evanston, Illinois 60208, USA*

Using e^+e^- collision data corresponding to 5.88×10^6 $\Upsilon(3S)$ [25.9×10^6 $\psi(2S)$] decays and acquired by the CLEO III [CLEO-c] detectors operating at CESR, we study the single-pion transitions from $\Upsilon(3S)$ [$\psi(2S)$] to the respective spin-singlet states $h_{b[c]}$. Utilizing only the momentum of suitably selected transition-π^0 candidates, we obtain the upper limit $\mathcal{B}(\Upsilon(3S) \to \pi^0 h_b) < 1.2 \times 10^{-3}$ at 90% confidence level, and measure $\mathcal{B}(\psi(2S) \to \pi^0 h_c) = (9.0 \pm 1.5 \pm 1.3) \times 10^{-4}$. Signal sensitivities are enhanced by excluding very asymmetric $\pi^0 \to \gamma\gamma$ candidates.

PACS numbers: 13.20.Gd, 13.25.Gv, 14.40.Pq

Hadronic transitions between heavy quarkonia states provide a rich tableau of opportunities for experimental and theoretical investigations [1]. Such transitions can supply important production mechanisms for the lower-lying state, thereby allowing measurement of its mass, width, and decay channels, and can also enable nonperturbative QCD calculations of transition rates to confront experiment. In particular, observation and exploration of the $b\bar{b}$ [$c\bar{c}$] spin-singlet states $h_{b[c]}$ have depended strongly upon hadronic transitions from vector quarkonia

produced in e^+e^- collisions. The $h_{b[c]}$ states[1] were both expected and measured to have masses near the spin-weighted averages of the respective spin-triplet states $\chi_{b[c]J}$. Observations of $\psi(2S) \to \pi^0 h_c$ were reported first by CLEO [2] and later by BESIII [3]. Evidence for $\Upsilon(3S) \to \pi^0 h_b$ has been reported by *BABAR* [4]. Charged dipion transitions from higher-lying vector states were first shown to produce h_c by CLEO [5] and, later, both $h_b(1P)$ and $h_b(2P)$ by Belle [6].

In this article we report on attempts to measure

---

* Now at: Pacific Northwest National Laboratory, Richland, WA 99352

[1] Throughout this article, lowest radial excitations are implied unless explicitly indicated.

the branching fractions for the isospin-violating single-π^0 transitions from $\Upsilon(3S)$ [$\psi(2S)$] to $h_{b[c]}$. Previously, BABAR [4] measured the product branching fraction $\mathcal{B}(\Upsilon(3S) \to \pi^0 h_b) \times \mathcal{B}(h_b \to \gamma\eta_b) = (3.0 \pm 1.1 \pm 0.7) \times 10^{-4}$, finding evidence for a signal with significance of 3σ, consistent with predictions $\mathcal{B}(\Upsilon(3S) \to \pi^0 h_b) \approx (1.0-1.6) \times 10^{-3}$ [7, 8] and $\mathcal{B}(h_b \to \gamma\eta_b) = 41\%$ [9]. Meanwhile, BESIII [3] measured $\mathcal{B}(\psi(2S) \to \pi^0 h_c) = (8.4 \pm 1.3 \pm 1.0) \times 10^{-4}$ (in conjunction with a simultaneously determined $\mathcal{B}(h_c \to \gamma\eta_c) = (54.3 \pm 6.7 \pm 5.2)\%$), compatible with both potential model estimates [10] and a non-relativistic effective field theory prediction [11] (see also [12]) which found charmed meson loop contributions to mass shifts to be atypically small.

The two data sets used in this work were collected in e^+e^- collisions at the Cornell Electron Storage Ring (CESR), at the center-of-mass energies of the $\Upsilon(3S)$ and $\psi(2S)$ resonances, corresponding to $(5.88 \pm 0.12) \times 10^6$ $\Upsilon(3S)$ decays [13] and $(25.9 \pm 0.5) \times 10^6$ $\psi(2S)$ decays [14]. Events were recorded using the CLEO III and CLEO-c detectors for $\Upsilon(3S)$ and $\psi(2S)$ datasets, respectively. Both configurations are equipped with an electromagnetic calorimeter consisting of 7784 thallium-doped cesium iodide crystals and covering 93% of solid angle, initially installed in the CLEO II [15] detector configuration. The energy resolution of the crystal calorimeter is 5% (2.2%) for 0.1 GeV (1 GeV) photons. Calorimeter angular resolution is $\sim$10 (5) mrad at $E_\gamma = 100$ MeV (1 GeV), and does not significantly contribute to $\gamma\gamma$ mass resolution for the soft π^0 candidates considered in this analysis. The CLEO III tracking system [16] consists of a silicon strip vertex detector and a large drift chamber; a six-layer wire vertex detector replaced the silicon in the CLEO-c configuration [17]. The trackers achieve charged particle momentum resolutions of 0.35% and 0.6% at 1 GeV/c in 1.5 T and 1.0 T axial magnetic fields, respectively.

In both studies we demand the presence of only the transition pion (via $\pi^0 \to \gamma\gamma$) in hadronic events, and impose no restriction on the $h_{b[c]}$ decay other than the global event selections described later. Branching fractions for $h_{b[c]} \to \gamma\eta_{b[c]}$ are known to be large, so that $h_{b[c]}$ searches can and do reasonably seek to require either the radiative photon and/or a reconstructed $\eta_{b[c]}$; we avoid such an approach here. Instead, the magnitude of the $h_{b[c]}$ signal is inferred from the size of any enhancement in the distribution of $M_{\rm rec}(\pi^0)$, the mass recoiling against the putative transition π^0 ($M_{\rm rec}(\pi^0) \equiv \sqrt{(p_{res} - p_{\pi^0})^2}$ where p_{res} and p_{π^0} are the initial $\Upsilon(3S)[\psi(2S)]$ and the π^0 four-momenta, respectively). The main challenge is to design selection criteria to simultaneously preserve signal strength while suppressing the unavoidably large backgrounds.

We determine our selection criteria and fit procedure based on Monte Carlo (MC) simulations of resonance decays, continuum ($e^+e^- \to \gamma^* \to q\bar{q}$) background, and an off-resonance sample, 20.7 pb^{-1} taken $\sim$16 MeV/c^2 below the $\psi(2S)$, so as to avoid bias. The MC generation utilizes EvtGen [18], the values shown in Ta-

TABLE I. Four key values used in each MC-based optimization of selection criteria and some related energies of interest.

Item	Units	$\Upsilon(3S)$	$\psi(2S)$
$M(h_{b[c]})$	MeV/c^2	9900.0	3525.28
$\Gamma(h_{b[c]})$	MeV/c^2	0	0.86
$\mathcal{B}(h_{b[c]} \to \gamma\eta_{b[c]})$	%	38.0	37.7
$\mathcal{B}(\pi^0 h_{b[c]})$	10^{-4}	16	8.4
$E_{\pi^0}(\pi^0 h_{b[c]})$	MeV	446	159
$E_\gamma(\gamma\chi_{b[c]2,1})$	MeV	433, 452	128, 171

ble I, and the most recent relevant branching fraction, mass, and width measurements [13, 19, 20] and predictions (where measurements do not exist), followed by a GEANT-based simulation [21] of the two detector configurations. First, global event selections for $\Upsilon(3S)$ and $\psi(2S)$ are performed (with 92% and 95% efficiencies) as in Refs. [13] and [22], respectively. In order to isolate reliably-triggered resonance decays and suppress e^+e^-, $\mu^+\mu^-$, and $\tau^+\tau^-$ final states, the selections demand that there be well-reconstructed charged particle tracks and that the total measured energy in each event be consistent with that of the initial e^+e^- state. The copious background from $\psi(2S) \to \pi^+\pi^- J/\psi$ is reduced by requiring that events have no oppositely-charged pair of particles with dipion recoil mass near that of J/ψ.

We reconstruct the transition $\pi^0 \to \gamma\gamma$ candidates based on pairs of showers in the calorimeter that are not matched to the projected trajectory of any charged particle. Showers must be located well within the boundaries of the crystal calorimeter barrel ($|\cos\theta| < 0.81$) for $\psi(2S) \to \pi^0 h_c$, or barrel and endcaps ($0.85 < |\cos\theta| < 0.93$) for $\Upsilon(3S) \to \pi^0 h_b$, where θ is the polar angle with respect to the positron beam direction. Also, the showers must have $E_\gamma > 30(50)$ MeV in the barrel (endcap) calorimeter. To reduce background from non-photon hadron-induced showers, photon candidates are also required to have a lateral shower profile consistent with that of an isolated electromagnetic shower. Defining the π^0 mass "pull" ($\equiv (M_{\gamma\gamma} - M_{\pi^0})/\Delta M_{\gamma\gamma}$, where $\Delta M_{\gamma\gamma}$ is the photon-energy-dependent resolution on $\gamma\gamma$ invariant mass, typically $\sim$5-7 MeV/c^2), we find that restricting the mass pull to $[-3.0, +2.5]$ optimizes sensitivity to signal. The asymmetric mass pull range accounts for the presence of a low-side tail in $M_{\gamma\gamma}$ caused by lateral and longitudinal shower leakage from the crystals assigned to the photon candidate's shower. If a daughter photon is shared with more than one π^0 candidate, the pair with smaller mass pull is chosen. We then kinematically constrain $M_{\gamma\gamma}$ to the known M_{π^0} to improve π^0 momentum resolution.

By the very nature of such an inclusive measurement, most of our selected events will be background, and any inference of an $h_{b[c]}$ signal depends strongly on two char-
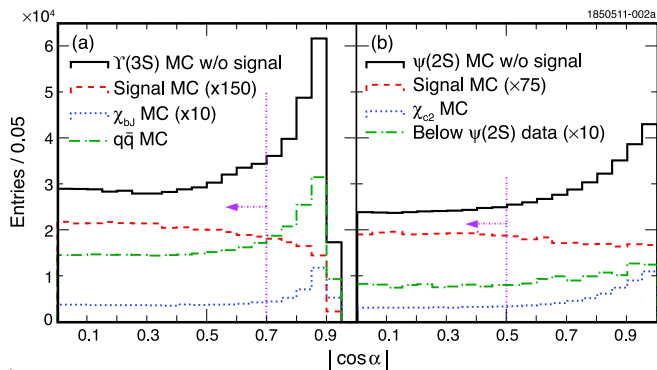
FIG. 1. Distributions of the π^0 decay angle α for MC (or data, where noted below) samples scaled to the size of our datasets: (a) $\Upsilon(3S) \rightarrow \pi^0 h_b$ signal (dashed), all $\Upsilon(3S)$ MC decays except signal (solid), $\Upsilon(3S) \rightarrow \gamma\chi_{bJ}$ (dotted), and $e^+e^- \rightarrow \gamma^* \rightarrow q\bar{q}$ (dash-dot), for $9875 < M_{\rm rec}(\pi^0) < 9925$ MeV/c^2; (b) $\psi(2S) \rightarrow \pi^0 h_c$ signal (dashed), all $\psi(2S)$ decays except signal (solid), $\psi(2S) \rightarrow \gamma\chi_{cJ}$ (dotted), and below-$\psi(2S)$ continuum data (dash-dot), for $3520 < M_{\rm rec}(\pi^0) < 3530$ MeV/c^2. Vertical lines and arrows show selected regions of $|\cos\alpha|$.

acteristics of the background: first, that it has smooth $M_{\rm rec}(\pi^0)$ dependence in the vicinity of the $h_{b[c]}$ mass, so that extrapolation of its shape underneath any signal can be made with confidence, and second, that its magnitude can be reduced enough to observe a peak of adequate statistical significance. Enormous combinatoric smooth backgrounds are present from $\pi^0 \rightarrow \gamma\gamma$ and $\eta \rightarrow \gamma\gamma$, which can arise from $e^+e^- \rightarrow q\bar{q}$ or at various stages of resonance transitions or decays. Although without structure in $M_{\rm rec}(\pi^0)$, these must be suppressed without sacrificing too much signal. Moreover, significant non-smooth structures in $M_{\rm rec}(\pi^0)$ are necessarily present as well. Because the spin-singlet masses are near the spin-weighted averages of the respective spin-triplet states, the transition-π^0 energy is always close to the photon energies from the electric-dipole (E1) transitions $\Upsilon(3S)[\psi(2S)] \rightarrow \gamma\chi_{b[c]J}$, as shown in Table I. An E1 photon will frequently be paired with one of the multitude of very low energy photons in most events to form a mass close to that of a true π^0. As the above-mentioned E1 photons are monochromatic, non-smooth contributions in $M_{\rm rec}(\pi^0)$ can arise near the $h_{b[c]}$ mass. These sources of fake π^0 candidates make extrapolating a reliably known background shape underneath any $h_{b[c]}$ signal systematically challenging unless mitigating measures are taken.

Our chosen method for fake-π^0 background suppression is to restrict the values of the $\pi^0 \rightarrow \gamma\gamma$ decay angle α, taken as the angle in the π^0 center-of-mass frame between either photon and the π^0-boost direction. True π^0 decays have a uniform distribution in $|\cos\alpha|$. Values of $|\cos\alpha|$ near unity imply an asymmetric decay, with one of the photons being very soft; it is these candidates which give rise to most of the background. MC studies
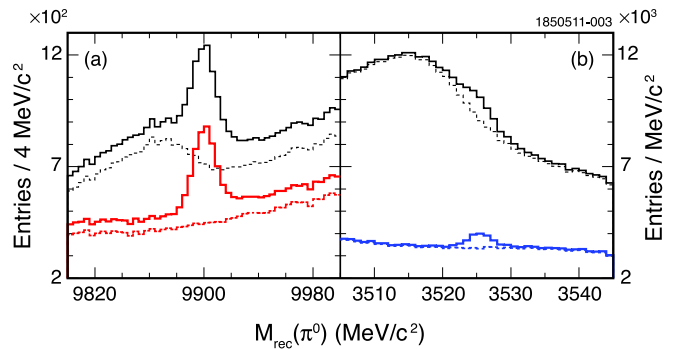

FIG. 2. Solid histograms show distributions in $M_{\rm rec}(\pi^0)$ for MC samples of signal $\pi^0 h_{b[c]}$ transitions at modeled levels plus (a) $\gamma\chi_{bJ}$, and (b) $\gamma\chi_{c2}$ backgrounds, scaled to the size of our datasets, with our restrictions on π^0 decay angle [(a) $|\cos\alpha| < 0.7$, (b) < 0.5] (lower pairs of histograms) and with $|\cos\alpha| < 1.0$ (upper pairs). Dashed histograms show the contribution of (a) $\gamma\chi_{bJ}$, and (b) $\gamma\chi_{c2}$-only events for both selections on $|\cos\alpha|$.

TABLE II. Features of the fits for signal extraction. "Order" in background shapes refers to order of polynomials. See text for other details.

Item	$\Upsilon(3S)$	$\psi(2S)$
$M_{\rm rec}(\pi^0)$ binning	4 MeV/c^2	1 MeV/c^2
$M_{\rm rec}(\pi^0)$ fit range	9.8-10.0 GeV/c^2	3505-3545 MeV/c^2
Background shape	3$^{\rm rd}$-order	ARGUS+2$^{\rm nd}$-order
$M(h_{b[c]})$ for fit	9900 MeV/c^2	3525.42 MeV/c^2
Signal shape	Reversed CBL	Double Gaussian

indicate that $|\cos\alpha| < 0.7$ [0.5] provides the best compromise between sensitivity and background rejection for $\Upsilon(3S) \rightarrow \pi^0 h_b$ [$\psi(2S) \rightarrow \pi^0 h_c$]. The tighter value for $\psi(2S) \rightarrow \pi^0 h_c$ reflects the order-of-magnitude larger values of $\mathcal{B}(\psi(2S) \rightarrow \gamma\chi_{cJ})/\mathcal{B}(\psi(2S) \rightarrow \pi^0 h_c)$ relative to $\mathcal{B}(\Upsilon(3S) \rightarrow \gamma\chi_{bJ})/\mathcal{B}(\Upsilon(3S) \rightarrow \pi^0 h_b)$ and the consequent need to suppress the $\gamma\chi_{cJ}$ backgrounds more severely. All these points are demonstrated in Figs. 1 and 2, where it can be seen that backgrounds congregate at larger $|\cos\alpha|$ and cause structure in $M_{\rm rec}(\pi^0)$ unless suppressed. The signal histograms in Fig. 1 fall with increasing $|\cos\alpha|$ due to the requirement that $E_\gamma > 30(50)$ MeV in the barrel (endcap) calorimeter, the $M_{\rm rec}(\pi^0)$ range restriction for these plots, and other event selection criteria. Exclusion of asymmetric $\pi^0 \rightarrow \gamma\gamma$ decays also has the advantage of improving $M_{\rm rec}(\pi^0)$ resolution (which enhances sensitivity) because such decays include softer photons, which have poor relative energy resolution.

Signal extraction is accomplished by fitting each $M_{\rm rec}(\pi^0)$ distribution with suitable binning and range for the combination of smooth background and peaking signal component shapes with fixed $M(h_{b[c]})$ and floating normalizations for each; choices of mass, binning,

range, and shapes appear in Table II. The h_b signal shape is found to be best represented by a reversed Crystal Ball line (CBL) shape (an ordinary CBL shape [23] with the power-law tail on the high side) while fixing the shape parameters based on signal-only fits to MC samples. A third-order polynomial for the h_b background fits the data well. The h_c shape is chosen instead as a double Gaussian with independent means (the mean of the broader Gaussian is shifted higher) based on studies of our signal MC sample. The different signal shapes reflect those expected for very slow (h_c) and faster (h_b) π^0 mesons, and reflect that the calorimeter resolution is more symmetric at lower energies and develops a low-side tail at higher energies due to shower leakage; the tail moves to the high side in recoil mass. Since E_{π^0} from $\psi(2S) \rightarrow \pi^0 h_c$ is close to the kinematic limit of $M(\pi^0)$, the h_c background shape is represented by an ARGUS function [24], which effectively models reduced phase space as a function of increasing mass, plus a second-order polynomial. Our MC studies show we can extract branching fractions consistent with what we input to the MC samples with these fit procedures.

Results from the fits appear in Figs. 3 and 4 and Table III. No signal is seen for $\Upsilon(3S) \rightarrow \pi^0 h_b$, and the quoted upper limit integrates over physical branching fractions only and includes systematic effects (see below). An unambiguous signal is observed for $\psi(2S) \rightarrow \pi^0 h_c$. The data points above the fit level near 3513 MeV/c^2 in Fig. 4(b) have a width narrower than the detector resolution, and hence must constitute a statistical fluctuation. The statistical significances shown are computed as $\sqrt{-2 \ln (L_{wo}/L_w)}$, where L_{wo} and L_w are likelihood values from fits of $M_{rec}(\pi^0)$ without and with signal shape components, respectively. If the h_c mass is allowed to float, 3525.9 ± 0.3 MeV/c^2(a mass value 1.1σ larger than the world average [19]) is obtained which results in negligible change in fitted yields with respect to the case when the mass is fixed to the world average. The final branching fractions are obtained as $\mathcal{B} = N_{evt}/(\epsilon N_{res})$ where N_{evt} is the number of signal events extracted from the fit, N_{res} is the number [13, 14] of resonance decays in the dataset, and ϵ is the reconstruction efficiency obtained from performing similar fits on MC samples.

We consider a variety of sources for systematic uncertainties on the branching fractions obtained from the fits, and summarize them in Table IV along with estimates of their contributions. The general approach is to vary the important selection criteria or fitting choices over reasonable ranges and note any resulting variations in $\mathcal{B}(\Upsilon(3S)[\psi(2S)] \rightarrow \pi^0 h_{b[c]})$ beyond expected statistical changes, and then to add all such effects in quadrature. The dominant systematic effects are quite different for h_b and h_c. For h_b, the source that stands out is the $M_{rec}(\pi^0)$ fit range. For h_c, the largest contributions come from the functional form of the background shape, uncertainty in $\Gamma(h_c)$, and our understanding of π^0 resolution in data and MC simulation. As $M_{rec}(\pi^0)$ resolutions are larger than the $h_{b[c]}$ mass uncertainties [3, 4, 6, 19], there is no
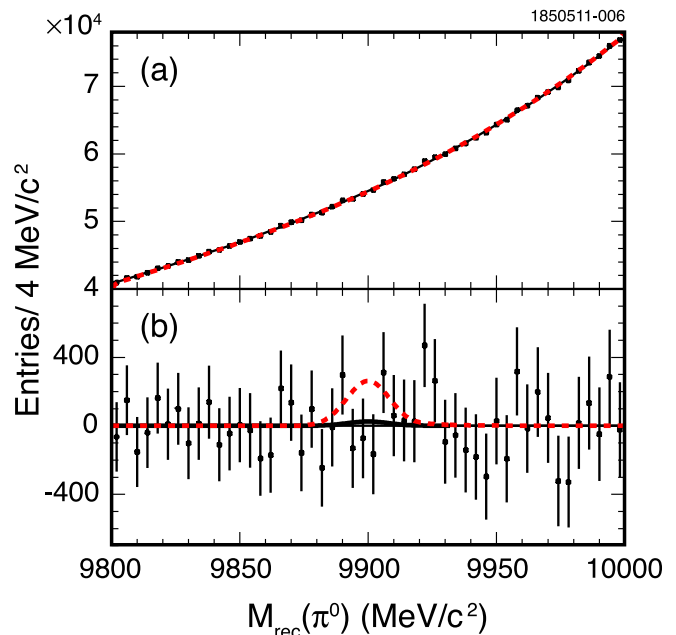

FIG. 3. (a) Fit to $M_{rec}(\pi^0)$ for $\Upsilon(3S) \rightarrow \pi^0 h_b$ for fixed $M(h_b) = 9900.0$ MeV/c^2. The χ^2 value from this fit is 26.4 for 50 data points (minus 5 parameters) with confidence level of 98.8%. (b) The fitted background-subtracted spectrum (solid curve). The dashed curve corresponds to the upper limit on signal candidates at 90% CL (< 1439 events or $\mathcal{B}(\Upsilon(3S) \rightarrow \pi^0 h_b) < 11 \times 10^{-4}$ @ 90% CL).

TABLE III. Signal-extraction efficiencies and final measured event yields and branching fractions, the latter including systematic uncertainties. The upper limit integrates over physical values only. See text for details.

Item	$\Upsilon(3S)$	$\psi(2S)$
$\epsilon(\pi^0 h_{b[c]})$	21.3%	12.6%
N_{evt}	139 ± 821	2943 ± 501
Significance	0.2σ	5.9σ
$N_{res}(10^6)$	5.88 ± 0.12	25.9 ± 0.5
$\mathcal{B}(\pi^0 h_{b[c]})$ (10^{-4})	< 12 @90% CL	$9.0 \pm 1.5 \pm 1.3$

need for separate systematic errors from such variation.

For the h_b $M_{rec}(\pi^0)$ fit range, we consider alternate ranges 50 MeV/c^2 wider and narrower, symmetrically around our chosen $M(h_b)$, observing excursions as large as noted in Table IV. For background shape, a fourth-order polynomial is tried instead of a third-order; for signal shape, we allow a double Gaussian instead of the reversed CBL shape (effects of imperfectly understood $M_{rec}(\pi^0)$ resolution are also accounted for in this variation). To test the dependency of our result upon the predicted resolution in $M_{rec}(\pi^0)$, we decrease the smearing predicted by the MC by 8.5% less than predicted (which no longer gives reasonable agreement between data and
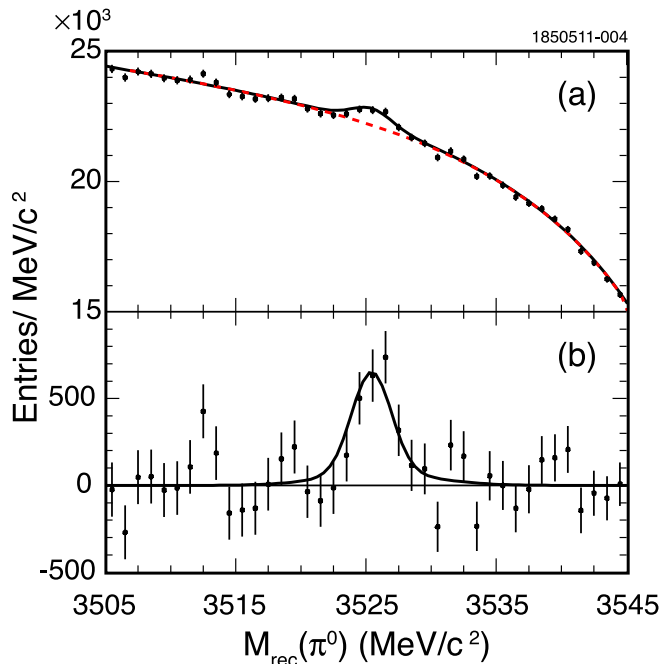
FIG. 4. (a) Fit to the $\psi(2S) \to \pi^0 h_c$ $M_{\mathrm{rec}}(\pi^0)$ data with (solid curve) and without (dashed) a signal. The χ^2 value from this fit is 41.0 for 40 data points (minus 5 parameters) with confidence level of 22.5%. (b) As in (a) but with the background fit from (a) subtracted.

range (3505–3550 MeV/c^2; we could not go lower than 3505 MeV/c^2 due to the contamination from $\psi(2S) \to \gamma\chi_{c2}$), suppression of events from $\psi(2S) \to \pi^+\pi^- J/\psi$, bin width (1±0.5) MeV/$c^2$, as well as doubling and halving the assumed $\mathcal{B}(h_c \to \gamma\eta_c)$, which includes the value measured by BESIII [3].

In conclusion, we have measured branching fractions for $\Upsilon(3S)[\psi(2S)] \to \pi^0 h_{b[c]}$ as shown in Table III. The h_b upper limit is dominated by statistical uncertainties and

TABLE IV. Summary of relative systematic uncertainties in percent on $\mathcal{B}(\Upsilon(3S) \to \pi^0 h_b)$ and $\mathcal{B}(\psi(2S) \to \pi^0 h_c)$. Entries marked "–" make negligible contributions.

Source	h_b	h_c
Background shape	0.8	9.3
$\Gamma(h_{b[c]})$	–	7.8
Fit range	19.7	–
Binning	10.9	–
Signal shape	1.7	–
π^0 resolution	2.0	6.6
N_{res}	2.0	2.0
$\mathcal{B}(h_{b[c]} \to \gamma\eta_{b[c]})$	2.5	4.1
Efficiency (MC statistics)	0.4	0.6
$|\cos\alpha|$	–	–
Quadrature sum	22.9	14.6

MC samples), and consider half of the change in its measured branching fraction as a possible systematical bias. For binning of $M_{\mathrm{rec}}(\pi^0)$, we vary from 4 to both 2 and 6 MeV/c^2 for h_b. We allow $\mathcal{B}(h_b \to \gamma\eta_b)$ to vary from 0% and up to 100% because its size is unknown and has a small but nonzero effect on photon multiplicity and therefore upon the efficiency of the signal π^0 reconstruction. We also account for the uncertainty in N_{res}.

For the $\psi(2S) \to \pi^0 h_c$ fit, the background shape is alternately fit to either first- or third-order polynomials instead of the second-order. The h_c signal size appears to have an approximately linear dependence on the assumed $\Gamma(h_c)$, behaving as $\mathcal{B}(\psi(2S) \to \pi^0 h_c) = [7.6 + 1.4\Gamma(h_c)/\Gamma_0] \times 10^{-4}$, where $\Gamma_0 = 0.86$ MeV/c^2 is the chosen width. We then vary the width by ±50% of 0.86 MeV/c^2 to estimate a systematic error. We account for uncertainty in calorimeter resolution by varying it over ranges that still represent the data reasonably well, as in our h_b study. We vary $|\cos\alpha|_{\mathrm{max}}$ (0.5±0.1), the fit

supersedes the previous CLEO limit, $\mathcal{B}[\Upsilon(3S) \to \pi^0 h_b] < 2.7 \times 10^{-3}$ at 90% CL [25]. If we combine the product branching fraction from BABAR [4] with our result, considering only physical values of branching fractions, we infer $\mathcal{B}(h_b \to \gamma\eta_b) > 21\%$ at 90% CL, consistent with predictions [9]. The h_c result is consistent with the value from BESIII [3].

ACKNOWLEDGMENTS

[1] N. Brambilla et al., Eur. Phys. J. C **71**, 1534 (2011).
[2] J. Rosner et al. (CLEO Collaboration), Phys. Rev. Lett. **95**, 102003 (2005); P. Rubin et al. (CLEO Collaboration), Phys. Rev. D **72**, 092004 (2005); S. Dobbs et al. (CLEO Collaboration), Phys. Rev. Lett. **101**, 182003 (2008).
[3] M. Ablikim et al. (BESIII Collaboration), Phys. Rev. Lett. **104**, 132002 (2010).
[4] J. P. Lees et al. (BABAR Collaboration), arXiv:1102.4565.
[5] R. E. Mitchell et al. (CLEO Collaboration), arXiv:1102.3424.
[6] I. Adachi et al. (Belle Collaboration), arXiv:1103.3419.

[7] M. B. Voloshin, Sov. J. Nucl. Phys. **43**, 1011 (1986); M. B. Voloshin and V. I. Zakharov, Phys. Rev. Lett. **45**, 688 (1980).

[8] U.G. Meißner, private communication.

[9] S. Godfrey and J. L. Rosner, Phys. Rev. D **66**, 014012 (2002).

[10] Y. P. Kuang, Phys. Rev. D **65**, 094024 (2002).

[11] F. -K. Guo, C. Hanhart, G. Li, U. -G. Meissner, Q. Zhao, Phys. Rev. D **82**, 034025 (2010).

[12] T. J. Burns, arXiv:1105.2533 [hep-ph].

[13] M. Artuso *et al.* (CLEO Collaboration), Phys. Rev. Lett. **94**, 032001 (2005).

[14] H. Mendez *et al.* (CLEO Collaboration), Phys. Rev. D. **78**, 011102 (2008).

[15] Y. Kubota *et al.* (CLEO Collaboration), Nucl. Instr. Meth. Phys. Res. Sect. A **320**, 66 (1992).

[16] D. Peterson *et al.*, Nucl. Instrum. Meth. A **478**, 142 (2002).

[17] R.A. Briere *et al.* (CLEO-c/CESR-c Taskforces & CLEO-c Collaboration), Cornell LEPP preprint CLNS 01/1742 (2001) (unpublished).

[18] D.J. Lange, Nucl. Instrum. Methods Phys. Res., Sect. A **462**, 152 (2001).

[19] K. Nakamura *et al.* (Particle Data Group), J. Phys. G **37**, 075021 (2010).

[20] M. Kornicer *et al.* (CLEO Collaboration), Phys. Rev. D **83**, 054003 (2011).

[21] R. Brun *et al.*, Geant 3.21, CERN Program Library Long Writeup W5013 (1993), unpublished.

[22] S. B. Athar *et al.* (CLEO Collaboration), Phys. Rev. D. **70**, 112002 (2004). Here, however, the maximum deposited energy in the calorimeter, E_{cal}, is loosened from 85% of the center-of-mass energy (E_{CM}) to 100%.

[23] J. E. Gaiser, Ph. D. Thesis, SLAC-R-255 (1982) (unpublished); T. Skwarnicki, Ph. D. Thesis, DESY-F31-86-02 (1986) (unpublished).

[24] H. Albrecht *et al.* (ARGUS Collaboration), Phys. Lett. B **241**, 278 (1990).

[25] F. Butler *et al.* (CLEO Collaboration), Phys. Rev. D **49**, 40 (1994).